JOURNAL OF THERMOPHYSICS AND HEAT TRANSFER
Vol. 18, No. 1, January–March 2004

Perturbation Solution to Mixed Convection in Rotating Horizontal Elliptic Cylinders

Olumuyiwa Ajani Lasode*
University of Ilorin, Ilorin 240003, Nigeria

A parameter perturbation analysis of laminar free and forced convective heat transfer in rotating horizontal elliptic ducts is investigated. The perturbation parameter used in the solution of the normalized governing equations is the rotational Rayleigh number Ra_τ, which governs rates of heating and rotation. The results show the influence of rotation and heating on the temperature and axial velocity fields. The effects of Prandtl number, in the range of 0.73 to 4, and eccentricity on the peripheral local Nusselt number are also reported. Results indicate insensitivity of peripheral local Nusselt number to Prandtl number at tube eccentricity $e = 0.866$, which is an important result to a designer of rotating heat exchanger. The effect of eccentricity on the friction coefficient is also presented. The parameter space for the overall validity of the results presented is $0 \le Ra_\tau \, Re_m \, Pr \le 640$.

Nomenclature

a, b	=	semimajor and semiminor axes of an ellipse, respectively
Cp	=	specific heat at constant pressure
e	=	eccentricity
$f\ (r, \theta)$	=	function specifying the temperature distribution in the (r, θ) plane
g	=	acceleration caused by gravity
H	=	distance between axis of rotation and tube axis
i	=	order of perturbation solution
k	=	thermal conductivity of the fluid
$Nu(\theta)$	=	peripheral local Nusselt number
O	=	tube axis
O'	=	center of the fixed frame of reference
$P\ (r, \theta)$	=	function specifying the pressure distribution in the (r, θ) plane
Pr	=	Prandtl number
p, P	=	elemental fluid/pressure distribution, respectively
R	=	dimensionless radius
Ra_τ	=	rotational Rayleigh number
Re_m	=	modified Reynolds number
Ro^*	=	Rossby number
r, r_b	=	any radial from center and to boundary, respectively
T, T_b	=	dimensional local and dimensional bulk temperatures, respectively
T_w	=	wall temperature
u, v, w	=	dimensional velocity in radial, azimuthal, and axial directions, respectively
W, Z	=	dimensionless axial velocity and distance in z direction, respectively
α	=	thermal conductivity
β	=	coefficient of thermal expansion
γ, τ	=	axial pressure and temperature gradients, respectively
ε_a	=	axes displacement parameter
η, η_b	=	dimensionless temperature and dimensionless bulk temperatures, respectively
θ	=	angle, deg
∇^2	=	Laplace operator
∇^4	=	biharmonic operator, $\nabla^2(\nabla^2)$
λ	=	angle between normal to the tangent and the horizontal
μ, ν	=	dynamic and kinematic viscosities, respectively
ξ	=	boundary coordinate
ρ	=	density of fluid
$\chi(\theta)$	=	form of the boundary coordinate, $\sqrt{\xi}$
ψ	=	streamfunction
Ω	=	angular velocity of tube

Received 19 August 2002; revision received 9 June 2003; accepted for publication 8 July 2003. Copyright © 2003 by the American Institute of Aeronautics and Astronautics, Inc. All rights reserved. Copies of this paper may be made for personal or internal use, on condition that the copier pay the $10.00 per-copy fee to the Copyright Clearance Center, Inc., 222 Rosewood Drive, Danvers, MA 01923; include the code 0887-8722/04 $10.00 in correspondence with the CCC.

*Lecturer, Department of Mechanical Engineering.

Introduction

THE power output from electrical machines is to some extent governed by the permissible temperature rise in the insulation surrounding the rotor conductors. Although cooling of these conductors is commonly achieved by the forced circulation of air over the rotor periphery, there are advantages to be gained if the heat transfer is effected through a suitable coolant flowing inside the conductors themselves especially for large machines such as those found in hydroelectric power stations. In practice axial cooling holes having a variety of cross-sectional shapes are commonly used. It is thus evident that the problem of forced flow through heated rotating channels is interesting both academically and practically.

Extensive research[1–9] has been carried out to study heat transfer and fluid flow in rotating and nonrotating coolant channels especially of the circular-type geometry, whereas research[10–12] carried out on elliptic geometry is limited to nonrotating systems. However, Bello-Ochende and Lasode[13] worked on rotating elliptic geometry. In his monograph Morris[2] cited a closely related work in which heated flow in circular-sectioned duct was studied using perturbation analysis adopting a power series solution up to first order for a horizontal duct rotating about a parallel axis. Several experimental works have been carried out to confirm the theoretical analyses of the flow process and heat transfer in rotating coolant channels of circular geometry, reported in various forms by Morris,[3] Morris,[4] Davies and Morris,[5] and Morris.[6]

Mori and Nakayama[7] studied theoretically fully developed laminar flowfield and temperature in a pipe rapidly rotating around a perpendicular axis by assuming velocity and temperature boundary layers along the pipe wall. It was shown that the resistance coefficient and the Nusselt number increased remarkably as a result of secondary flow driven by the Coriolis force. Siegel[8] analyzed laminar heat transfer in a tube rotating about an axis perpendicular to the tube axis for flow that is radially outward from the axis of rotation. Power series solution up to second order using the Taylor number as a perturbation parameter was constructed. Bello-Ochende[10] conducted a numerical study on natural convection in horizontal elliptic cylinders. He presented results for nonuniform heat-flux applications at the cylinder periphery in graphical forms for heat transfer and flow regimes for some values of eccentricity and a range of Rayleigh numbers.

In another work Bello-Ochende[11] studied the thermal problem of transition-point heat transfer for forced laminar convection in heated horizontal elliptic ducts, using the concept of scale analysis. Results he obtained indicate that in the neighborhood of eccentricity $e = 0.866$ optimum results are predicted for the generalized transition-point Nusselt number based on the major diameter and the corresponding generalized thermal entrance length for the parameter space, $0.75 \leq e < 1.0$.

Bello-Ochende and Lasode[13] studied laminar combined free- and forced-convection heat transfer in rotating horizontal elliptic ducts and presented results of heat transfer and fluid flow in graphical forms. Their results indicate that optimum heat transfer is predicted when the eccentricity $e = 0.433$. Faris and Viskanta[9] studied laminar combined forced-and free-convection heat transfer in a horizontal tube using a perturbation method. They presented approximate analytical solutions as well as average Nusselt numbers graphically for a range of Prandtl and Grashof numbers. Adegun[12] investigated laminar forced convective heat transfer in an inclined elliptic duct using scale and perturbation techniques. Thermal and hydrodynamic entrance problems were investigated using a scale approach while a perturbation approach was used to analyze the fully developed region of the duct. Useful results were obtained, among which are that for optimum heat transfer a critical aspect ratio of 0.5 ($e = 0.866$) is predicted and that perturbation results indicate a considerable effect of inclination on circular ducts and elliptic geometry of $e = 0.433$, whereas the effect is negligible for the configuration for $e = 0.866$.

The focus of the present study is an investigation of fully developed laminar forced-and free-convection heat transfer in horizontal elliptic ducts rotating about a parallel axis using a parameter perturbation technique. The technique is an approximate analytic method in which the normalized governing equations are expanded in power series using the rotational Rayleigh number Ra_τ, the dimensionless parameter governing the rates of heating and rotation. The effects of the perturbation parameter Ra_τ and modified Reynolds number on the temperature and axial velocity profiles are studied. The effects of Prandtl number on the peripheral local Nusselt number are investigated. The effects of eccentricity on friction coefficient are also examined.

Physical Problem and Mathematical Formulations

The physical model and the cylindrical polar coordinate (r, θ, z) system are shown in Fig. 1.

For the flow regime the following assumptions should be noted:

1) Laminar fully developed flow is considered.

2) Heated tube is treated, and the thermal conductivity of the tube material is high enough to smooth out circumferential variations in wall temperature.

3) The fluid temperature distribution can be mathematically stated as

$$T = \tau z + f(r, \theta) \tag{1}$$

because of the combined assumptions of fully developed flow and uniform axial heating. Equation (1) is applicable at the wall, meaning that the wall temperature will increase uniformly in the direction of flow. At any axial location the difference in wall temperature T_w and

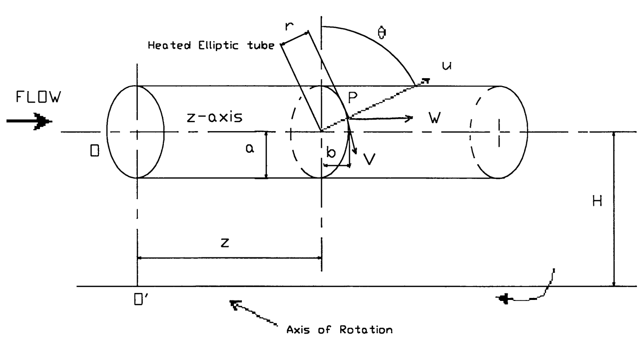

Fig. 1 Physical model, coordinate axes, and regions of the duct.

any local value of temperature in the flow will also be functionally related to the cross-stream coordinates.

4) Except for density, fluid properties are taken to be constant with temperature.

5) Because distances far away from inlet effects are being considered, the pressure distribution must be of the form

$$P = \gamma z + P(r, \theta) \tag{2}$$

6) It is assumed that there are no chemical reactions, no heat sources within the fluid, radiation is neglected, and viscous dissipation is ignored.

The following nondimensionalization parameters are adopted for the dependent and independent variables:

$$R = \frac{r}{a}, \qquad Z = \frac{z}{a}, \qquad W = \frac{w}{a}, \qquad \eta = \frac{T_w - T}{\tau a Pr}$$

$$v = -\nu\left(\frac{\partial \psi}{\partial r}\right), \qquad u = \frac{\nu}{r}\left(\frac{\partial \psi}{\partial \theta}\right) \tag{3}$$

The normalized governing equations are as follows:

Normalized streamfunction equation:

$$\nabla^4\psi + \frac{1}{R}\frac{\partial(\psi, \Delta^2\psi)}{\partial(R, \theta)} + Ra_\tau\left(\frac{1}{R}\frac{\partial \eta}{\partial \theta}\cos\theta + \frac{\partial \eta}{\partial R}\sin\theta\right)$$

$$+ \frac{Ra_\tau}{\varepsilon_a}\frac{\partial \eta}{\partial \theta} + \frac{Ra_\tau * Ro^*}{Re_m}\cdot\frac{1}{R}\frac{\partial(\eta, \psi)}{\partial(R, \theta)} = 0 \tag{4}$$

where

$$\nabla^4\psi = \nabla^2(\nabla^2\psi) \tag{5}$$

Equation (5) is the biharmonic operator.

Normalized axial velocity equation:

$$\nabla^2 W + \frac{1}{R}\frac{\partial(\psi, W)}{\partial(R, \theta)} + 4Re_m = 0 \tag{6}$$

Normalized energy transport equation:

$$\nabla^2\eta + \frac{Pr}{R}\cdot\frac{\partial(\psi, \eta)}{\partial(R, \theta)} + W = 0 \tag{7}$$

The normalization procedure adopted highlights the following dimensionless groups that govern this problem.

Rotational Rayleigh number:

$$Ra_\tau = \frac{\Omega^2 H\beta\tau a^4}{\alpha\nu}$$

Rossby number:

$$Ro^* = -a^2 2H\Omega\rho\nu\cdot\frac{\partial P}{\partial z}$$

Modified Reynolds number:

$$Re_m = \frac{-a^3}{4\rho\nu^2}\cdot\frac{\partial p}{\partial z}$$

Axes displacement parameter:

$$\varepsilon_a = a/H$$

Prandtl number:

$$Pr = \nu/\alpha$$

Solution Technique

The normalized governing equations are solved using a series expansion in ascending powers of the rotational Rayleigh number Ra_τ. This asymptotic series expansion is truncated at the second order and therefore presents an approximate solution. This technique was successfully used by Morton[14] and Morris.[4] The need for the satisfaction of the boundary conditions for different polar coordinates at the boundary of the ellipse needs the consideration of the eccentricity e and the angular position θ. For the derivation of the boundary coordinate ξ, the parametric equations of an ellipse are invoked.

$$\xi = \left(\frac{r_b}{a}\right)^2 = \frac{(1-e^2)}{(1-e^2\cos^2\theta)} \tag{8}$$

Boundary Conditions

The normalized boundary constraints are as follows:

1) $\psi = W = \eta = 0$ at $R = \sqrt{\xi}$, that is, at the boundary.

2) $\psi = W = \eta \neq 0$ (that is, finite) at $R = 0$, that is, at the core of the duct.

3) $\partial\psi/\partial R = 1/R$. $\partial\psi/\partial\theta = 0$ at $R = \sqrt{\xi}$, and $\partial\psi/\partial R = 1/R$. $\partial\psi/\partial\theta \neq 0$ (that is, finite) at the centre of the elliptic duct.

The parameter perturbation technique adopted in the solution of the problem gave rise to the power series representation of the normalized governing equations, which is expanded with rotational Rayleigh number Ra_τ as follows:

1) Streamfunction:

$$\psi = \sum_{i=0}^{n} Ra_\tau^i \psi_i = \psi_0 + Ra_\tau \psi_1 + Ra_\tau^2 \psi_2 + \cdots \tag{9}$$

2) Axial velocity:

$$W = \sum_{i=0}^{n} Ra_\tau^i W_i = W_0 + Ra_\tau W_1 + Ra_\tau^2 W_2 + \cdots \tag{10}$$

3) Temperature:

$$\eta = \sum_{i=0}^{n} Ra_\tau^i \eta_i = \eta_0 + Ra_\tau \eta_1 + Ra_\tau^2 \eta_2 + \cdots \tag{11}$$

Substituting Eqs. (9–11) into Eqs. (4), (6), and (7), respectively, it is possible, upon integrating the resulting cascade of differential equations and application of the boundary constraints, to arrive at the following solutions.

Zeroth-Order Solution

1) Zeroth-order streamfunction:

$$\psi_0 = 0 \tag{12}$$

There can be no flow in the (r, θ) plane when $Ra_\tau = 0$ as a result of the absence of circulation or secondary flow. This corresponds to a no-heating condition.

2) Zeroth-order axial velocity:

$$W_0 = Re_m(\xi - R^2) \tag{13}$$

3) Zeroth-order temperature:

$$\eta_0 = (Re_m/16)[3\xi^2 - 4\xi R^2 + R^4] \tag{14}$$

First-Order Solution

1) First-order streamfunction:

$$\psi_1 = \frac{\sin\theta Re_m}{4608} \cdot R(10\xi^3 - 21\xi^2 R^2 + 12\xi R^4 - R^6) \tag{15}$$

2) First-order axial velocity:

$$W_1 = \frac{Re_m^2 \cos\theta}{184{,}320} \cdot R[49\xi^4 - 100\xi^3 R^2 + 70\xi^2 R^4 - 20\xi R^6 + R^8] \tag{16}$$

3) First-order temperature:

$$\eta_1 = \frac{Re_m^2 \cos\theta}{22{,}118{,}400}[(381 + 1325Pr)\xi^5 R - (735 + 3000Pr)\xi^4 R^3 + (500 + 2600Pr)\xi^3 R^5 - (175 + 1125Pr)\xi^2 R^7 + (30 + 210Pr)\xi R^9 - (1 + 10Pr)R^{11}] \tag{17}$$

Second-Order Solution

1) Second-order streamfunction: The final solution contains numerical coefficients of an unwieldy nature; therefore, they have been grouped within summation signs and the values tabulated in Table A1 (see Appendix).

$$\psi_2 = \frac{Re_m^2 \sin 2\theta}{4608^2}\left\{\sum_{r=1}^{2}\left[C_{(2r-1)} + D_{(2r-1)}Pr\right]\xi^{(7\frac{1}{2}-r)}R^{(2r-1)} + \sum_{r=3}^{7}(C_{2r} + D_{2r}Pr)\xi^{(7-r)}R^{2r}\right\} + \frac{Re_m^2 \sin\theta}{22{,}118{,}400\varepsilon_a}\left\{\sum_{s=0}^{7}\left[C_{(2s+1)} + D_{(2s+1)}Pr\right]\xi^{(7-s)}R^{(2s+1)}\right\} + \frac{Ro^* \cdot Re_m \cos\theta}{18{,}432}\left[\sum_{t=0}^{6} C_{(2t+1)}\xi^{(6-t)}R^{(2t+1)}\right] \tag{18}$$

2) Second-order axial velocity (see Table A2 in the Appendix for actual value of coefficients):

$$W_2 = \frac{Re_m^3 \cos 2\theta}{(4608)^2}\left\{\sum_{r=1}^{3}\left[E_{(2r-1)} + F_{(2r-1)}Pr\right]\xi^{(8\frac{1}{2}-r)}R^{(2r-1)} + \sum_{r=4}^{10}\left[E_{2(r-2)} + F_{2(r-2)}Pr\right]\xi^{(10-r)}R^{2(r-2)}\right\} - \frac{Re_m^3 \cos\theta}{1{,}159{,}200\varepsilon_a}\left\{\sum_{s=0}^{8}\left[E_{(2s+1)} + F_{(2s+1)}Pr\right]\xi^{(8-s)}R^{(2s+1)}\right\} + \frac{Ro^* \cdot Re_m^2 \sin\theta}{9216}\left[\sum_{t=0}^{7} F_{(2t+1)}\xi^{(7-t)}R^{(2t+1)}\right] + \frac{Re_m^3}{(4608)^2}\left[-1.3572\xi^{7\frac{1}{2}}R + \sum_{x=1}^{8} E_{2x}\xi^{(8-x)}R^{2x}\right] \tag{19}$$

3) Second-order temperature (see Table A3 in the Appendix for actual value of coefficients):

$$\eta_2 = \frac{Re_m^3 \cos 2\theta}{(4608)^2}\left\{\sum_{r=1}^{4}\left[L_{(2r-1)} + M_{(2r-1)}Pr + N_{(2r-1)}Pr^2\right] \times \xi^{(9\frac{1}{2}-r)}R^{(2r-1)} + \sum_{r=5}^{12}\left[L_{2(r-3)} + M_{2(r-3)}Pr + N_{2(r-3)}Pr^2\right]\xi^{(12-r)}R^{2(r-3)}\right\} + \frac{Re_m^3 \cos\theta}{22{,}118{,}400\varepsilon_a} \times \left\{\sum_{s=0}^{9}\left[L_{(2s+1)} + M_{(2s+1)}Pr + N_{(2s+1)}Pr^2\right]\xi^{(9-s)}R^{(2s+1)}\right\} + \frac{Re_m^3}{(4608)^2}\left\{\sum_{t=1}^{2}\left[L_{(2t-1)} + M_{(2t-1)}Pr + N_{(2t-1)}Pr^2\right] \times \xi^{(9\frac{1}{2}-t)}R^{(2t-1)} + \sum_{t=3}^{11}\left[L_{2(t-2)} + M_{2(t-2)}Pr + N_{2(t-2)}Pr^2\right]\xi^{(11-t)}R^{2(t-2)}\right\} - \frac{Ro^* \cdot Re_m^2 \sin\theta}{73{,}728} \times \left\{\sum_{x=0}^{8}\left[L_{(2x+1)} + M_{(2x+1)}Pr\right]\xi^{(8-x)}R^{(2x+1)}\right\} \tag{20}$$

Because the resulting algebra is extremely tedious, only details for solutions up to the second order are presented. The contribution of the second-order term to the entire solution is less than 10% and not more accurate result could be justified by the amount of effort required to include more terms. The overall validity range of the results presented is obtained following the continuation procedure suggested by Tormcej and Nandakumar[15] in which the bisection method is incorporated.

Peripheral Local Nusselt Number

The Nusselt number is a dimensionless quantity indicative of the rate of energy convection from the surface. For the conduction-referenced heat transfer with respect to the bulk temperature and considering the normal temperature gradient, we have the peripheral local Nusselt number as

$$Nu(\theta) = \frac{2}{\eta_b} \frac{\partial \eta}{\partial R}\bigg|_{R=\chi(\theta)} \cos(\lambda - \theta) \tag{21}$$

where

$$\eta_b = \frac{\int_0^{2\pi} \int_0^{\chi(\theta)} \eta(R,\theta) W(R,\theta) R \,\mathrm{d}R \,\mathrm{d}\theta}{\int_0^{2\pi} \int_0^{\chi(\theta)} W(R,\theta) R \,\mathrm{d}R \,\mathrm{d}\theta} \tag{22}$$

and

$$\chi(\theta) = \sqrt{\xi} \tag{23}$$

Friction Coefficient

The normalized form of the friction coefficient (the parameter indicating the influence of rotation on the established resistance to flow using the Blasius friction factor) is given by

$$C_{\mathrm{fr}} = \frac{4\pi^2(1-e^2)Re_m}{\left[\int_0^{2\pi} \int_0^{\chi(\theta)} W R \,\mathrm{d}R \,\mathrm{d}\theta\right]^2} \tag{24}$$

Discussion of Results

Figures 2a and 2b present the effect of modified Reynolds number on temperature and axial velocity distribution respectively, across tube diameter for a circular tube ($e = 0.0$) for solutions up to the second-order for the range of operating parameters shown on each figure. It can be seen that the positions of maximum values of temperature and axial velocity vary slightly with changes in the modified Reynolds number Re_m for a particular value of the rotational Rayleigh number Ra_τ. However, the maximum values for the temperature and axial velocity increase significantly with increases in the modified Reynolds number Re_m.

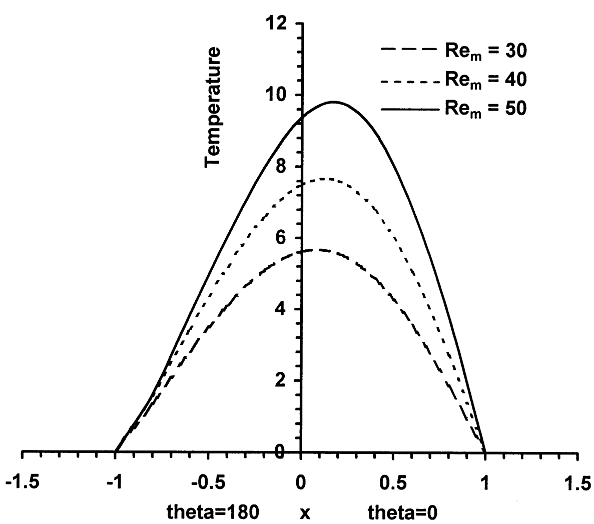

a) Temperature

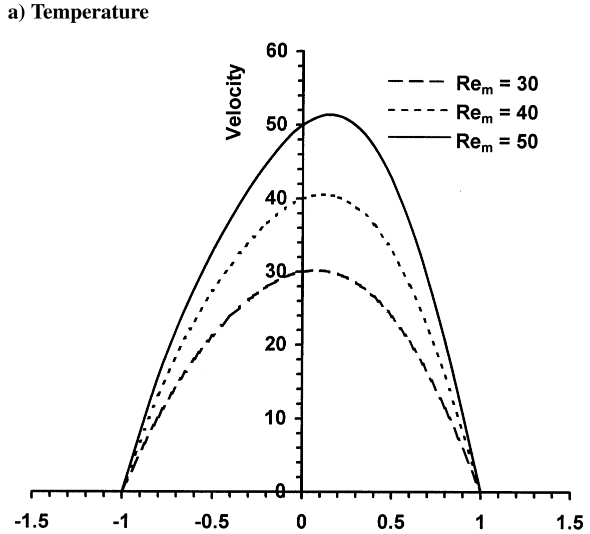

b) Axial velocity

Fig. 2 Effect of modified Reynolds number on temperature and axial velocity distribution: Ra_T = 10, Pr = 0.73, Ro^* = 1, ε_a = 1/48, and e = 0.

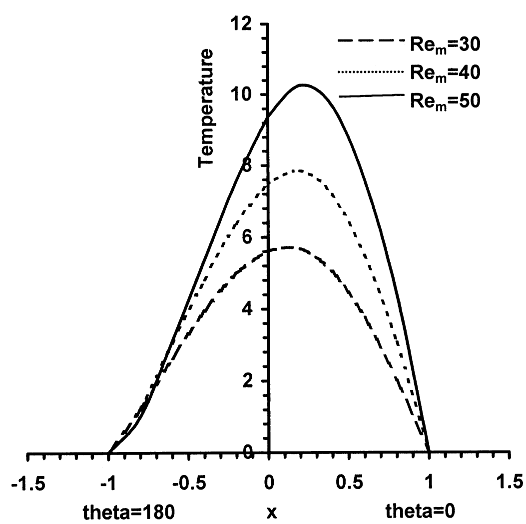

a) Temperature

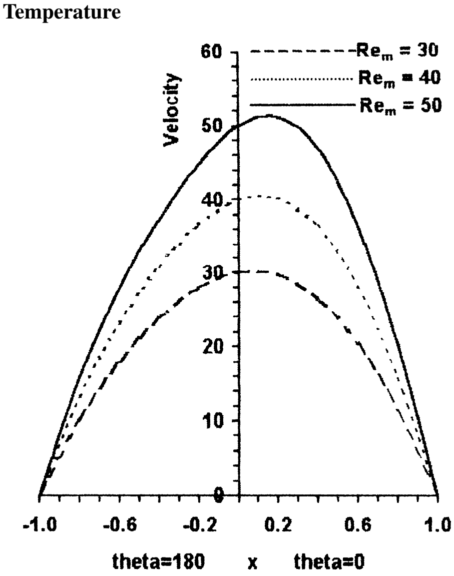

b) Axial velocity

Fig. 3 Effect of modified Reynolds number on temperature and axial velocity distribution: Ra_T = 10, Pr = 1, Ro^* = 1, ε_a = 1/48, and e = 0.433.

These results differ from the results obtained by Morris[4] in which he focused on fluid flowing in a vertical tube rotating about a parallel axis, whereas the present analysis focuses on fluid flowing in a horizontal elliptic tube rotating about a parallel axis. The difference in both analyzes can be attributed to the gravitational effects on temperature and axial velocity profiles, which is typical of fluid flowing in a vertical tube and hence must be included in that analysis.

Figures 3a and 3b present the effect of modified Reynolds number on temperature and axial velocity distribution, respectively, across the major diameter up to the second-order solution for an elliptic tube of eccentricity $e = 0.433$ with the stated set of operating parameters.

The general lateral shifts in the temperature and velocity profiles away from the origin, caused by the influences of heating and rotation, are noticeable. Increases in the modified Reynolds number Re_m result in corresponding increases in the maximum values of the local temperature or axial velocity as the case might be. The effect of increased eccentricity and consequent boundary deformation is noticeable on the profile of temperature and axial velocity plots especially for $Re_m = 50$.

Figures 4a and 4b show the effect of the rotational Rayleigh number Ra_τ on temperature distribution across major diameter and minor diameter, respectively, up to the second-order solution for elliptic tube $e = 0.433$. From Fig. 4a it can be observed that increase in the rotational Rayleigh number Ra_τ, which is a measure of rate of heating and rotation, results in gradual shift of points of maximum value in temperature profiles away from the origin and a corresponding increase in the maximum value of the local temperature. The secondary flow increases correspondingly, and the temperature profiles become distinctly different from those of pure convection. This result is similar to the findings of Faris and Viskanta.[9]

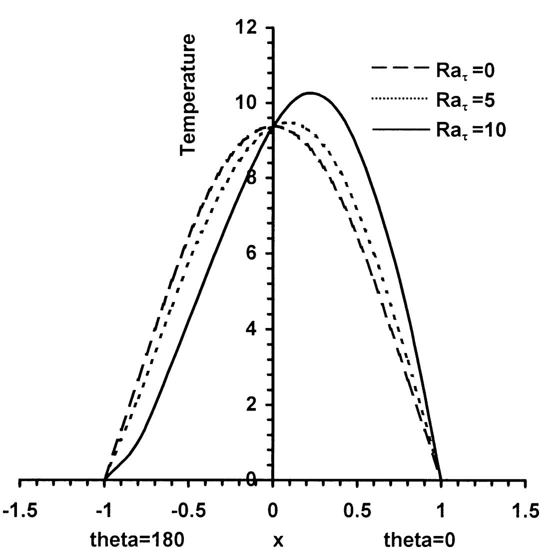

a) Major diameter

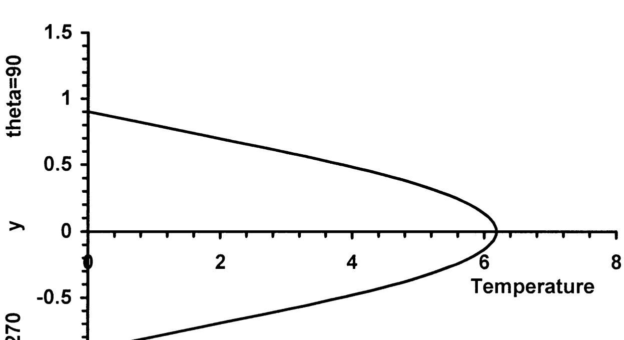

b) Minor diameter

Fig. 4 Effect of rotational Rayleigh number on temperature distribution: Re_m = 50, Pr = 1, Ro^* = 1, ε_a = 1/48, and e = 0.433.

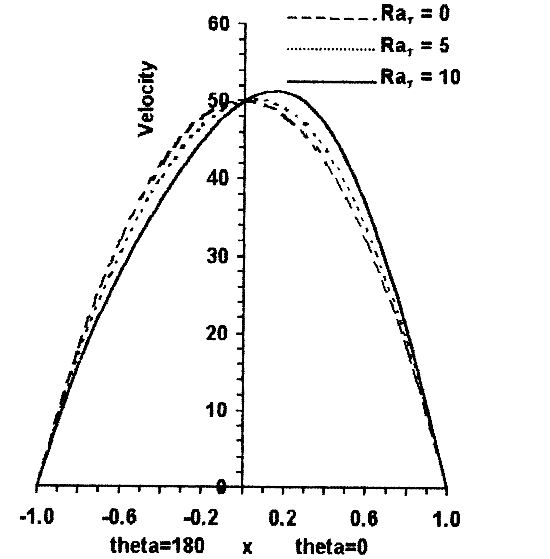

a) Major diameter

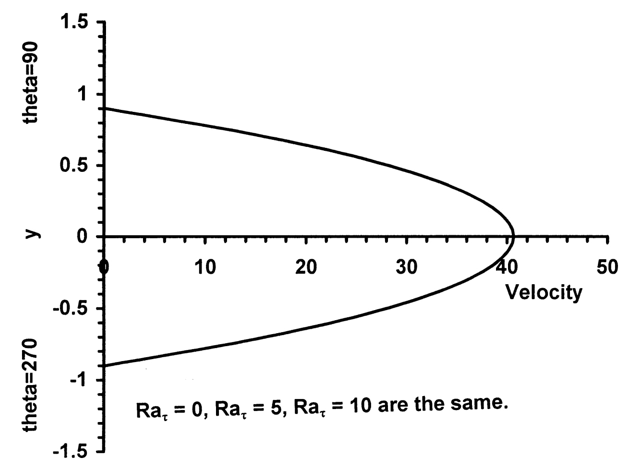

b) Minor diameter

Fig. 5 Effect of rotational rayleigh number on axial velocity distribution: Re_m = 50, Pr = 1, Ro^* = 1, ε_a = 1/48, and e = 0.433.

However, Fig. 4b shows that along the minor diameter an increase in the rotational Rayleigh number Ra_τ does not result in any change in the temperature profile, and the curve is symmetrical about a center of the elliptic duct. The first- and second-order components, which perturbed the zeroth order, are insignificantly small when computed along the minor diameter. This result confirms that, based on heuristic reasoning, the effect of bouyancy forces caused by free convection might be insignificant along the minor diameter.

Figures 5a and 5b show the effect of the rotational Rayleigh number Ra_τ on axial velocity distribution across major diameter and minor diameter, respectively, up to the second-order solution for elliptic tube $e = 0.433$. Figure 5a indicates that as the rotational Rayleigh number Ra_τ increases then the more pronounced is the deformation of the axial velocity profile and its deviation from the parabolic nature for no-heating condition. Furthermore, the general shift in the profile away from the origin is noticeable, with increase in the maximum local value as a result of bouyancy forces. Adegun[12] made a similar observation in his work in which a nonrotating system was considered. However, Fig. 5b shows that increases in the rotational Rayleigh number Ra_τ does not have significant

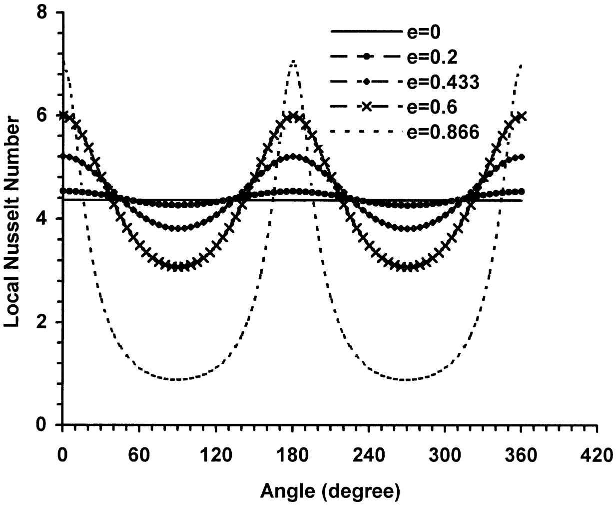

a) **Rotational Rayleigh number, Ra_T = 0**

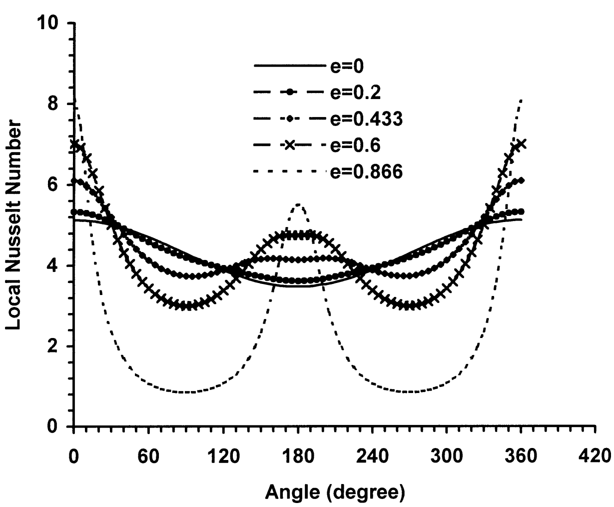

b) **Rotational Rayleigh number, Ra_T = 10**

Fig. 6 Effect of eccentricity on local Nusselt number: Re_m = 50, Pr = 1, Ro^* = 1, and ε_a = 1/48.

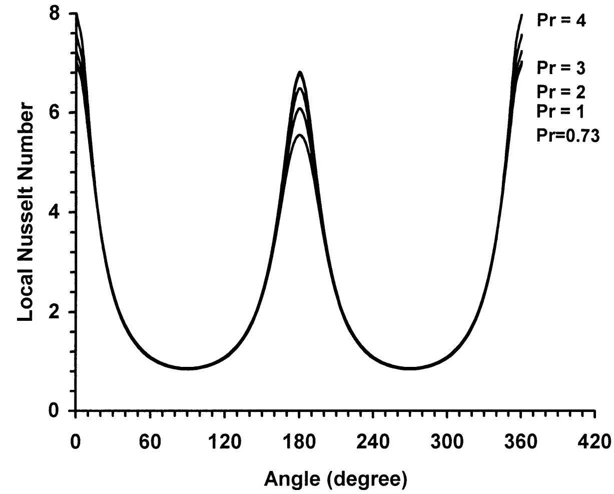

Fig. 7 Effect of Prandtl number on local Nusselt number at e = 0.866: Ra_T = 5, Re_m = 30, Ro^* = 1, and ε_a = 1/48.

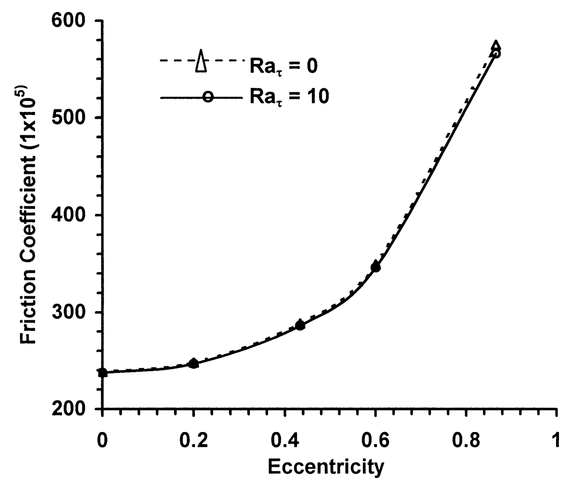

Fig. 8 Effect of eccentricity on friction coefficient: Re_m = 50, Pr = 1, Ro^* = 1, and ε_a = 1/48.

effects on the parabolic profile for no heating condition (that is, $Ra_\tau = 0$).

Figures 6a and 6b show the effect of duct eccentricity on peripheral local Nusselt number at various angular positions under no-heating cum no-rotation $Ra_\tau = 0$ and heating and rotation $Ra_\tau = 10$ conditions, respectively. Figure 6a shows oscillations of the peripheral local Nusselt number about the value $Nu(\theta) = 4.364$ (the value predicted for circular tube $e = 0.0$ undergoing pure forced convection) as the eccentricity increases above zero. The highest value occurrs at angular positions 0 deg, 180 deg, and 360 deg, while the minimum values are at 90 deg and 270 deg. Figure 6b reveals that because of the effects of heating and rotation the degree of oscillations of the peripheral local Nusselt number reduces. This might also be attributable to the influence of bouyancy forces and secondary flow.

Moreover, Fig. 7 shows the effect of Prandtl number Pr on the peripheral local Nusselt number for elliptic duct ($e = 0.866$). It reveals that the peripheral local Nusselt number seems to be insensitive to changes in the Prandtl number Pr. This might be an important result for designer of rotating elliptic heat exchanger, who would like to use any available fluid as the heat-transfer fluid because Prandtl number is a property of fluid.

Figure 8 shows the plot of friction coefficient against tube eccentricity for no heating $Ra_\tau = 0$ and heating $Ra_\tau = 10$ conditions. The figure indicates monotonic increase in friction coefficient for both conditions. For the circular geometry ($e = 0.0$) the friction coefficient has a higher value for $Ra_\tau = 10$ compared to $Ra_\tau = 0$, which is in line with the findings of Morris.[2] However, for the elliptic ducts the numerical values of the friction coefficient for $Ra_\tau = 10$ are lower compared to the values for $Ra_\tau = 0$ showing heating and rotation reduce friction coefficient, though the two curves seems to merge.

Conclusions

The parameter perturbation technique used in this paper is valid for low values of the rotational Rayleigh number Ra_τ. At the fully developed flow region considered, $C_{fr} = \eta = W = Nu(\theta) = F(Ra_\tau, Re_m, Pr)$. The results show that the perturbation parameter Ra_τ is responsible for the lateral shift of the temperature and axial velocity profile away from the origin along the major diameter and its deviation from the usual parabolic profile associated with pure forced convection caused by secondary flow effects and bouyancy forces. Along the minor diameter these effects are insignificant. The results predict that the peripheral local Nusselt number is insensitive to Prandtl number changes for a duct of eccentricity $e = 0.866$. This is an important result for a designer of rotating heat exchanger. It is shown that the increase in modified Reynolds number manifests an increase in maximum values of temperature and axial velocity. These results are in agreement with the published works of Morris[2,4] and Faris and Viskanta[9] for rotating circular ducts, Bello-Ochende and Lasode[13] for rotating elliptic ducts, and Adegun[12] for nonrotating elliptic ducts.

Appendix A: Tables of Second-Order Perturbation Coefficients

Table A1 ψ_2 coefficients

ψ_2 coefficients		
r	$C_{(2r-1)}$	$D_{(2r-1)}$
1	1.3235	4.1401
2	−2.0295	−7.8261
r	C_{2r}	D_{2r}
3	0.1097	5.4857
4	0.9578	−2.2639
5	−0.3925	0.5195
6	0.0325	−0.057
7	−0.0015	0.0017
s	$C_{(2s+1)}$	$D_{(2s+1)}$
0	1.0332	3.3059
1	−2.4931	−8.1727
2	1.9844	6.9010
3	−0.6380	−2.6042
4	0.1302	0.6771
5	−0.0182	−0.1172
6	0.0015	0.0104
7	−0.0000	−0.0003
t	$C_{(2t+1)}$	
0	0.0436	
1	−0.1129	
2	0.1042	
3	−0.0451	
4	0.0117	
5	−0.0015	
6	0.0000	

Table A2 W_2 coefficients

W_2 coefficients		
r	$E_{(2r-1)}$	$F_{(2r-1)}$
1	0.3036	1.0358
2	−0.6618	−2.0701
3	0.3383	1.3045
r	$E_{2(r-2)}$	$F_{2(r-2)}$
4	0.0483	——
5	0.16	——
6	−0.2939	−0.3483
7	0.1330	0.0915
8	−0.0298	−0.0145
9	0.0024	0.0012
10	−0.0001	−0.0000
s	$E_{(2s+1)}$	$F_{(2s+1)}$
0	−0.0956	−0.1888
1	0.1292	0.4132
2	−0.1239	−0.3405
3	0.0413	0.1438
4	−0.008	−0.0326
5	0.0011	0.0056
6	−0.0001	−0.0007
7	0.0000	0.0000
8	−0.0000	−0.0000
t	$E_{(2t+1)}$	
0	−0.0025	
1	0.0055	
2	−0.0047	
3	0.0022	
4	−0.0006	
5	0.0001	
6	−0.0000	
7	0.0000	
x	E_{2x}	
1	4.0833	
2	−6.7633	
3	7.26	
4	−4.6333	
5	1.7298	
6	−0.3472	
7	0.0287	
8	−0.0008	

Table A3 η_2 coefficients

η_2 coefficients			
r	$L_{(2r-1)}$	$M_{(2r-1)}$	$N_{(2r-1)}$
1	0.019	0.1422	0.2842
2	−0.0380	−0.2949	−0.5175
3	0.0276	0.1984	0.4123
4	−0.0070	−0.0483	−0.0815
r	$L_{2(r-3)}$	$M_{2(r-3)}$	$N_{2(r-3)}$
5	——	0.0090	−0.0302
6	−0.0014	0.0051	0.1202
7	−0.0025	−0.0209	−0.2470
8	0.0030	0.0093	0.0996
9	−0.0009	0.0003	−0.0474
10	0.0002	−0.0002	−0.0079
11	−0.0000	0.0000	−0.0006
12	0.0000	−0.0000	−0.0000
s	$L_{(2s+1)}$	$M_{(2s+1)}$	$N_{(2s+1)}$
0	0.0075	0.0508	0.0856
1	−0.0149	−0.1118	−0.2066
2	0.0108	0.0971	0.2047
3	−0.0043	0.0478	−0.1145
4	0.0010	0.0138	0.0378
5	−0.0001	−0.0024	−0.0082
6	0.0000	0.0003	0.0014
7	−0.0000	−0.0000	−0.0002
8	0.0000	0.0000	0.0000
9	−0.0000	−0.0000	−0.0000
t	$L_{(2t-1)}$	$M_{(2t-1)}$	$N_{(2t-1)}$
1	−0.0119	−0.0894	−0.2993
2	0.1697	——	——
t	$L_{2(t-2)}$	$M_{2(t-2)}$	$N_{2(t-2)}$
3	——	0.2646	0.9201
4	−0.2722	−0.4264	−1.6063
5	0.1932	0.4466	1.8732
6	−0.1152	−0.2837	−1.3647
7	0.0468	0.1127	0.6305
8	−0.0121	−0.0283	−0.1802
9	0.0018	0.0042	0.0288
10	−0.0001	−0.0003	−0.0022
11	0.0000	0.0000	0.0001
x	$L_{(2x+1)}$	$M_{(2x+1)}$	
0	0.0013	0.0045	
1	−0.0025	−0.0109	
2	0.0018	0.0112	
3	−0.0008	−0.0067	
4	0.0002	0.0024	
5	−0.0000	−0.0006	
6	0.0000	0.0001	
7	−0.0000	−0.0000	
8	0.0000	0.0000	

References

[1]Holzworth, H., *Die Entwicklung der Holzworth—Gas Turbine*, Holzworth-Gas Turbinen, G.m.b.H Muehlmeim, Ruhr, Germany, 1938.

[2]Morris, W. D., *Heat Transfer and Fluid Flow in Rotating Coolant Channels*, Research Studies Press, Wiley, New York, 1981.

[3]Morris, W. D., "Heat Transfer Characteristics of a Rotating Thermosyphon," Ph.D. Dissertation, Mechanical Engineering, Univ. of Wales, Swansea, Wales, U.K., 1964.

[4]Morris, W. D., "Laminar Convection in a Heated Vertical Tube Rotating About a Parallel Axis," *Journal of Fluid Mechanics*, Vol. 21, Pt. 3, 1965, pp. 453–464.

[5]Davies, T. H., and Morris, W. D., "Heat Transfer Characteristics of a Closed Loop Rotating Thermosyphon," *Proceedings of the 3rd International Heat Transfer Conference*, Vol. 2, American Inst. of Chemical Engineers, Chicago, 1966, p. 172.

[6]Morris, W. D., "Terminal Laminar Convection in a Uniformly Heated Rectangular Duct," Inst. of Mechanical Engineers, Paper 4, 1968.

[7]Mori, Y., and Nakayama, W., "Convective Heat Transfer in Rotating Radial Circular Pipes," *International Journal of Heat and Mass Transfer*, Vol. 11, 1968, pp. 1027–1040.

[8]Siegel, R., "Analysis of Bouyancy Effect on Fully Developed Laminar Heat Transfer in a Rotating Tube," *Journal of Heat Transfer*, Vol. 107, Aug. 1985, pp. 338–344.

[9]Faris, G. N., and Viskanta, R., "An Analysis of Laminar Combined Forced and Free Convective Heat Transfer in a Horizontal Tube," *International Journal of Heat and Mass Transfer*, Vol. 12, 1969, pp. 1295–1309.

[10]Bello-Ochende, F. L.,"A Numerical Study of Natural Convection in Horizontal Elliptic Cylinders," *Revista Brasiliera de Ciencias Mecanicas*, Vol. 7, No. 4, 1985, pp. 353–371.

[11]Bello-Ochende, F. L., "Scale Analysis of Entrance Region Heat Transfer for Forced Convection in Elliptic Duct," *Proceedings of 11th RBCM Mechanical Engineering Conference*, Revista Brasiliera de Ciencias Mecanicas, Sao Paulo, Brazil, 1991.

[12]Adegun, I. K., "Analytic Studies of Convective Heat Transfer in Inclined Elliptic Ducts," M.E. Thesis, Dept. of Mechanical Engineering, Univ. of Ilorin, Ilorin, Nigeria, 1992.

[13]Bello-Ochende, F. L., and Lasode, O. A., "Convective Heat Transfer in Horizontal Elliptic Ducts in Parallel Mode Rotation," *International Journal of Heat and Technology*, Vol. 13, No. 1, 1995, pp. 105–122.

[14]Morton, B. R., "Laminar Convection in Uniformly Heated Horizontal Pipes at Low Rayleigh Numbers," *Quarterly Journal of Mechanics and Applied Mathematics*, Vol. 12, 1959, p. 410.

[15]Tormcej, R., and Nandakumar, K., "Mixed Convective Flow of a Power Law Fluid in Horizontal Duct," *The Canadian Journal of Chemical Engineering*, Vol. 64, 1986, p. 743.

Elements of Spacecraft Design

Charles D. Brown, *Wren Software, Inc.*

This new book is drawn from the author's years of experience in spacecraft design culminating in his leadership of the Magellan Venus orbiter spacecraft design from concept through launch. The book also benefits from his years of teaching spacecraft design at University of Colorado at Boulder and as a popular home study short course.

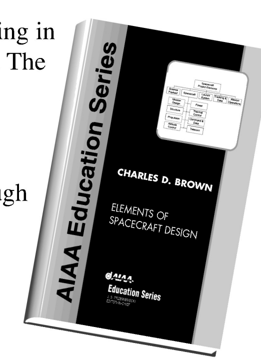

The book presents a broad view of the complete spacecraft. The objective is to explain the thought and analysis that go into the creation of a spacecraft with a simplicity and with enough worked examples so that the reader can be self taught if necessary. After studying the book, readers should be able to design a spacecraft, to the phase A level, by themselves.

Everyone who works in or around the spacecraft industry should know this much about the entire machine.

Table of Contents:

❖ Introduction
❖ System Engineering
❖ Orbital Mechanics
❖ Propulsion
❖ Attitude Control
❖ Power System
❖ Thermal Control
❖ Command And Data System
❖ Telecommunication
❖ Structures
❖ Appendix A: Acronyms and Abbreviations
❖ Appendix B: Reference Data
❖ Index

AIAA Education Series
2002, 610 pages, Hardback • ISBN: 1-56347-524-3 • List Price: $104.95 • **AIAA Member Price: $74.95**

American Institute of Aeronautics and Astronautics
Publications Customer Service, P.O. Box 960, Herndon, VA 20172-0960
Fax: 703/661-1501 • Phone: 800/682-2422 • E-mail: warehouse@aiaa.org
Order 24 hours a day at www.aiaa.org

AIAA
American Institute of Aeronautics and Astronautics

02-0547